UC Irvine
UC Irvine Previously Published Works

Title
Analytical and experimental study of turbulent methane-fired backmixed combustion

Permalink
https://escholarship.org/uc/item/9tp735vv

Journal
AIAA Journal, 15(5)

ISSN
0001-1452

Authors
Peck, RE
Samuelsen, GS

Publication Date
1977-05-01

DOI
10.2514/3.7358

Copyright Information

Peer reviewed

angles $\phi=0$ and $45°$ (Figs. 1a, 1b), however, there is very little difference between the computed results obtained by either procedure; as ϕ increases, so does the difference as shown in Figs. 1c and 1d.

A note should be made of the discrepancies in the temperature and velocity profiles at $\phi=135°$. Because of the relatively high angle of attack, the flow beyond about $\phi=120°$ is subject to adverse pressure gradient, which eventually leads to separation defined by zero shear stress component normal to the generator. Although our calculations with either procedure predict separation at about $\phi=161°$, close to the measured value of $\phi=159°$, the measured boundary layer shows a more rapid thickening than is predicted by calculations. This can be traced to vortex formation, in which case the ordinary boundary-layer equations are no longer valid anyway.

In summary we conclude that the similarity variable proposed by Bradshaw for turbulent flows over tapered wings is also applicable to the calculation of high Reynolds number turbulent boundary layer on cones at incidence with local similarity assumptions.

Although the improvements obtained by the "new" procedure may seem small in comparison with the empiricism contained in eddy-viscosity laws and viscous/inviscid interaction effects, they are nevertheless encouraging that the local similarity will work for other similar shapes as well. In principle, the procedure is strictly applicable to conical bodies with arbitrary cross-section provided that the radial pressure gradient is very small.

The computer time (CPU) for the present case with 1894 net points in the cross-flow plane was 7.86 sec (0.0042 sec/net point) on an IBM 370/165 computer.

References

[1] Cebeci, T. and Smith, A. M. O., *Analysis of Turbulent Boundary Layers*, Academic Press, New York, 1974.

[2] Cebeci, T., "Calculation of Three-Dimensional Boundary Layers, I. Swept Infinite Cylinders and Small Cross Flow," *AIAA Journal*, Vol. 12, June 1974, pp. 779-786.

[3] Cebeci, T., Calculation of Three-Dimensional Boundary Layers, II. Three-Dimensional Flows in Cartesian Coordinates," *AIAA Journal*, Vol. 13, Aug. 1975, pp. 1056-1064.

[4] Cebeci, T. and Abbott, D. E., "Boundary Layers on Rotating Disk," *AIAA Journal*, Vol. 13, June 1975, pp. 829-832.

[5] Adams, J. C., Jr., "Three-Dimensional Compressible Turbulent Boundary Layers on a Sharp Cone Incidence in Supersonic Flow," *International Journal of Heat and Mass Transfer*, Vol. 17, May 1974, pp. 581-595.

[6] Bontoux, P. and Roux, B., "Compressible Turbulent Boundary Layer on a Yawed Cone," *AIAA Journal*, Vol. 14, May 1976, pp. 545-546.

[7] Bradshaw, P., Mizner, C. A., and Unsworth, K., "Calculations of Compressible Turbulent Boundary Layers on Straight-Tapered Swept Wings," *AIAA Journal*, Vol. 14, March 1976, pp. 399-400.

[8] Cebeci, T., Kaups, K., and Rehn, J. A., "Some Problems of the Calculation of Three-Dimensional Boundary-Layer Flows on General Configurations," NASA CR-2285, July 1973.

[9] Bradshaw, P., Mizner, G. A., and Unsworth, K., "Calculation of Compressible Turbulent Boundary Layers with Heat Transfer on Straight-Tapered Swept Wings," Imperical College Aero Rept. 75-04, May 1975.

[10] Keller, H. B. and Cebeci, T., "Accurate Numerical Methods for Boundary Layers. II. Two-Dimensional Turbulent Flows," *AIAA Journal*, Vol. 10, Sept. 1972, pp. 1197-1200.

[11] Rainbird, W. J., "Turbulent Boundary-Layer Growth and Separation on a Yawed Cone," *AIAA Journal*, Dec. 1968, pp. 2140-2146.

Analytical and Experimental Study of Turbulent Methane-Fired Backmixed Combustion

R. E. Peck* and G. S. Samuelsen†
UCI Combustion Laboratory,
University of California, Irvine, Calif.

Nomenclature

D = combustor diameter
K = constant in effective viscosity expression
L = length of flowfield
r = radius
T = temperature
V = velocity
μ = viscosity
ρ = density
ϕ = equivalence ratio, $\dfrac{(F/A) \text{ actual}}{(F/A) \text{ stoichiometric}}$

I. Introduction

THE present results are from a continuing investigation designed to improve the prediction of reacting, recirculating flows and to clarify the mechanisms of pollutant formation in continuous combustion systems. The combustor configuration is a 51mm diameter axisymmetric duct containing an aerodynamic (opposed-jet) flameholder as shown in Fig. 1. The opposing, high-velocity jet stream serves to stabilize the flame by backmixing hot combustion products with fresh reactants (premixed methane/air).

The analytical model of the opposed-jet combustor (OJC) flowfield is founded on extended versions of the PISTEP method of Gosman et al.[1] The numerical procedure solves simultaneously the governing elliptic partial differential conservation equations with the corresponding dependent variables as follows: conservation of mass—stream function, ψ; conservation of momentum—vorticity, ω/r; conservation of energy—enthalpy, h; species continuity—mass fraction, m_j. A simplified effective viscosity model for turbulent momentum transport is adopted for the present investigation[1]:

$$\mu_{\text{eff}} = KD^{1/3} L^{1/3} \rho^{1/3} (\dot{m} V^2)^{1/3} \qquad (1)$$

Exchange coefficients for turbulent energy and mass transport are related to μ_{eff} by effective Prandtl and Schmidt numbers. The OJC geometry was initially incorporated into the computational procedure by Samuelsen and Starkman for an ammonia/air fired system.[2] A numerical solution for the methane/air system including the formation of the pollutant species CO and NO was later incorporated.[3] The present study compares the numerical prediction of local flowfield properties for the methane/air system with experimentally determined values.

II. Approach

Cold Flow

Consideration of cold flow conditions enables a preliminary evaluation of the transport models incorporated into the numerical procedure. The cold flow solution is ob-
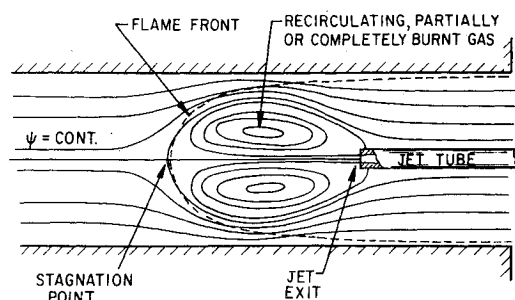
Fig. 1 Opposed-jet combustor schematic.

Fig. 2 Cold flow velocity profiles (•experimental; –predicted).

Fig. 3 Cold flow tracer concentration profiles.

tained by numerically solving the governing equations for the two dependent variables ψ, ω. The predicted spatial distributions of the time-average (mean) velocity are available for comparison to the experimental measurements. Pitot tube data for cold flow velocity are used as a reference base for evaluating the system hydrodynamics and the associated models of turbulence.

The effective mass exchange model is evaluated by considering an isothermal flowfield with a nonuniform concentration. The nonuniform concentration is established by introduction of a tracer into the jet. Spatial distributions of tracer concentrations are predicted numerically by solving an additional species conservation equation containing the appropriate mass exchange coefficient. Experimentally, a carbon monoxide (CO) tracer is introduced through the opposed-jet. Local CO concentrations are measured by NDIR analysis of gas samples extracted by conventional probing.

Reacting Flow

Calculated distributions of temperature and species mass fraction are compared to experimental results to assess the coupled models of turbulence and kinetics for the condition of reacting flow. The chemistry model incorporates kinetic mechanisms for methane, carbon monoxide, and nitric oxide.

A two-step quasi-global reaction mechanism is adopted for the methane oxidation[4]

$$CH_4 + O_2 \rightarrow CO + H_2O \qquad (2)$$

$$CO + O_2 \rightarrow CO_2 \qquad (3)$$
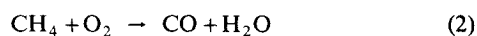
An initial solution for the reacting flowfield was obtained using published reaction rates that were later refined to more closely resemble the experimental data.

A detailed description of the numerical formulation of the reaction rate expressions may be found elsewhere.[3] The dependent variables for the hydrocarbon system include vorticity, ω/r, streamfunction, ψ, methane mass fraction, m_{CH_4}, carbon dioxide mass fraction, m_{CO_2}, and enthalpy, h. Distributions of other major species H_2O, CO and O_2 are related to m_{CH_4} and m_{CO_2} via elemental mass conservation.

Additional calculations were conducted to predict formation of the pollutant species, nitric oxide (NO). Nitrogen oxide kinetics were based on the familiar Zeldovich[5] mechanism:

$$O + N_2 \rightarrow NO + N \qquad (4)$$

$$N + O_2 \rightarrow NO + O \qquad (5)$$

Noting that reaction (4) is the rate limiting step simplifies the overall reaction rate to:

$$\frac{d[NO]}{dt} = 2k_4 [N_2] [O] \qquad (6)$$

The O-atom concentration in Eq. (6) was first calculated by assuming O/O_2 equilibrium and latter extended to consider
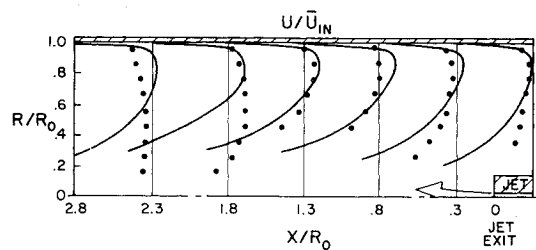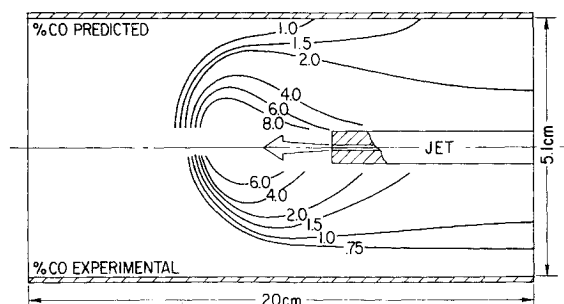
the "superequilibrium" of oxygen atoms following the method of Iverach et al.[6]

The experimental test conducted to complement the numerical predictions of OJC reacting flow properties utilized stoichiometric proportions of premixed methane/air in both the main and jet streams. Temperature and chemical composition measurements were obtained at the OJC exit plane. Temperature measurements were made using a Pt/Pt-13% Rh thermocouple. Gas samples were extracted via a water-cooled stainless steel probe and conveyed through a heated teflon sample line to a packaged exhaust gas analysis system. The instrumentation console provides quantitative analyses of CO and CO_2 (NDIR), NO/NO_x (chemiluminescence), total hydrocarbons (FID), and O_2 (paramagnetic).

III. Results and Discussion

Cold Flow

The cold flow studies were conducted for the following test conditions: approach velocity—$V_m = 7.62$ m/sec; jet velocity—$V_j = 130$ m/sec; temperature—$T_m = T_j = 294$ K; and equivalence ratio—$\phi_m = \phi_j = 0.0$. Experimental and predicted velocity profiles are presented in Fig. 2. The predicted velocity profiles agree qualitatively with experimental results. The predicted location of the stagnation point differs substantially from the location indicated experimentally. The intense mixing processes occurring in the recirculation zone suggest employing a refined model of turbulence which allows the turbulence length scale to vary throughout the flowfield. A thorough evaluation is currently limited by the experimental uncertainty of measurements in the highly turbulent shear layer between the jet and the main stream and in the recirculation zone itself.

Results of the tracer studies of mass transport in a turbulent, nonreacting flow are shown in Fig. 3. Although the reported trends are similar, the calculated tracer concentration profiles are quantitatively higher than those observed experimentally. These results demonstrate possible deficiencies in the mass exchange coefficient and more importantly in the simplified effective viscosity model used in the current study.

Reacting Flow

The conditions investigated for the reacting flow case were as follows: approach velocity—$V_m = 7.62$ m/sec; jet
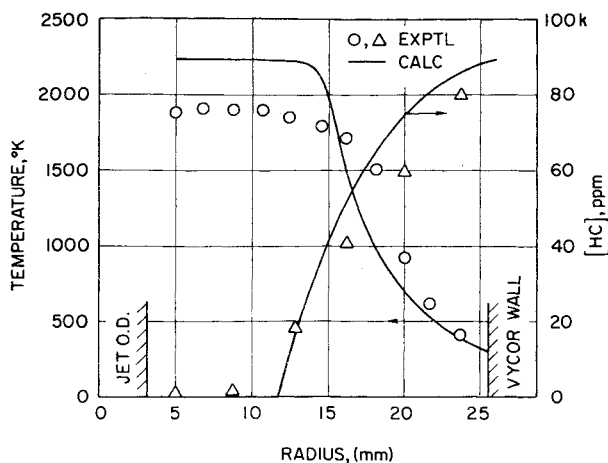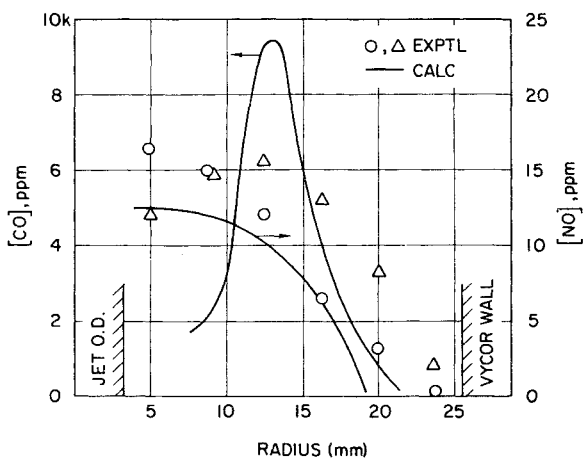
Fig. 4   OJC exhaust HC and temperature profiles.

Fig. 5   OJC exhaust CO and NO profiles.

velocity—$V_j = 130$ m/sec; temperature (inlet)—$T_m = T_j = 294$ K; and equivalence ratio—$\phi_m = \phi_j = 1.0$. Predictions of the spatial distribution of flowfield properties are presented in Ref. 3. The predicted location of the high temperature reaction zone begins immediately downstream of the stagnation point and parallels the jet wall to the exit plane with most of the fuel being consumed prior to exhaust. Exhaust plane measurements of temperature and hydrocarbon concentration are compared to predicted values in Fig. 4. The location of the flame front, indicated by sweep temperature and concentration gradients, coincides with theoretical predictions. The temperature deviation may be corrected by considering radiation losses in both the numerical and experimental results.

Fig. 5 presents similar results for CO and NO concentrations. Significant CO concentrations persist throughout the flame zone and reach a maximum in the transition (flame front) region where the temperature and oxygen concentration are relatively low. The indicated trends are favorable, although a sharper peak is predicted for the CO concentration profile than is observed experimentally. This result demonstrates the need to improve the specification of boundary conditions near solid walls as well as the basic chemistry model. The numerically predicted NO profiles indicate that the maximum concentrations appear in the peak temperature zone. The nonequilibrium O-atom calculations yield a 30-fold increase in NO production.

IV. Conclusions

Numerical predictions of the turbulent, backmixed flowfield of a methane-fired opposed-jet combustor have been compared to experimental observations. Although favorable qualitative correlation has been established, a cold flow analysis identified deficiencies in the simplified turbulence model considered and a reacting flow analysis identified deficiencies in the coupled turbulence/kinetic models adopted. The results from this preliminary study provide direction for further experimental verification and formulation of refined kinetic and transport mechanisms.

References

[1]Gosman, A. D., Pun, W. M., Runchal, A. K., Spalding, D. B., and Wolfshtein, M., *Heat and Mass Transfer in Recirculating Flows*, Academic Press, London, 1969.

[2]Samuelsen, G. S. and Starkman, E. S., "Analytical and Experimental Investigation of an Ammonia/Air Opposed Reacting Jet," *Combustion Science and Technology*, Vol. 5, 1972, pp. 31-41.

[3]Samuelsen, G. S. and Peck, R. E., "Pollutant Formation in Reacting Flow with Recirculation," Paper WSS/CI 72-21, *1972 Fall Meeting, Western States Section/The Combustion Institute*, Monterey, Ca., 1972.

[4]Williams, G. C., Hottel, H. C., and Morgan, A. C., "The combustion of Methane in a Jet-Mixed Reactor," *Twelfth Symposium (International) on Combustion*, The Combustion Institute, Pittsburgh, Pa., 1969, pp. 913-925.

[5]Zeldovich, Y. B., Sadovnikov, P. Y., and Kamenetski, D. A., "The Oxidation of Nitrogen by Combustion," Academy of Sciences of USSR, Institute of Chemical Physics, Moscow-Leningrad, 1947.

[6]Iverach, D., Basden, K. S., and Kirov, N.Y., "Formation of Nitric Oxide in Fuel-Lean and Fuel-Rich Flames," *Fourteenth Symposium (International) on Combustion*, The Combustion Institute, Pittsburgh, Pa., 1973, pp. 767-775.

Parametric Differentiation Technique Applied to a Combustion Problem

A.G. Marathe* and V.K. Jain†
Indian Institute of Science, Bangalore, India

Nomenclature

A_i	= constants of complementary solutions
B	= parameter depending on system considered
$C_i(Y,x)$	= complementary solutions of linear differential
$C_i(Z,x)$	equations
D_I	= first Damkohler number
m_I	= concentration of fuel
m_2	= concentration of oxidant
$P(Y,x)$ $P(Z,x)$	= particular solutions of linear differential equations
Pr	= Prandtl number
r	= stoichiometric ratio
Sc	= Schmidt number
T_a	= nondimensional activation energy
T_n	= nondimensional temperature
x	= similarity coordinate
Y	= rate variation of m_2 with respect to a parameter
Z	= rate variation of T_n with respect to a parameter

Subscripts

$\pm \infty$	= values at $\pm \infty$
$'$	= derivative with respect to x